18TH WORLD CONFERENCE ON EARTHQUAKE ENGINEERING
WCEE2024
MILAN
MILAN, ITALY
30TH JUNE - 5TH JULY 2024
www.wcee2024.it

STRUCTURAL HEALTH MONITORING OF A FULL-SCALE MASONRY BUILDING PROTOTYPE USING SMART BRICKS

A. Meoni[1], A. D'alessandro[2], M. Mattiacci[2], G. Virgulto[3], N. Buratti[3] & F. Ubertini[2]

[1] Department of Civil and Environmental Engineering, University of Perugia, Perugia, Italy, andrea.meoni@unipg.it

[2] Department of Civil and Environmental Engineering, University of Perugia, Perugia, Italy

[3] Department of Civil, Chemical, Environmental, and Materials Engineering, University of Bologna, Bologna, Italy

Abstract: *Smart bricks are innovative clay-based strain sensors for Structural Health Monitoring (SHM) of masonry constructions. Their shape and size resemble that of conventional bricks, yet internally the clay matrix is suitably modified through the addition of a metallic filler to boost their piezoresistive response. Smart bricks are therefore capable of outputting measurable changes in their electrical resistance when mechanically strained under compression. An electromechanical model is adopted to convert the electrical outputs from each sensor into strain measurements. Smart bricks can be placed at strategic positions within the load-bearing structure of a masonry construction to monitor changes in strain due to damage initiation and propagation. They can be internally deployed within walls, arches, and pillars by forming both dense and coarse sensor networks, thus enabling different SHM strategies. Their use covers the monitoring of the most common structural pathologies affecting masonry constructions, including damages caused by differential settlements, material aging, excessive loading, and earthquakes. The paper presents an experimental campaign in which smart bricks are used to monitor strain within a full-scale masonry building prototype. The specimen is subjected to controlled damage of increasing intensity under real environmental conditions. Preliminary results obtained by testing the structure are presented and discussed to demonstrate the effectiveness of smart bricks in measuring strain in such a realistic structural setting.*

1. Introduction

Masonry buildings often possess significant cultural and historical value that deserves long-term preservation. Factors such as the aging of building materials, insufficient maintenance, exposure to unexpected loading conditions, and natural hazards, such as earthquakes and ground settlements, can negatively impact the structural performance of existing masonry buildings during their service life, jeopardizing the safety conditions of occupants and the historical value possessed by the structures themselves. Under these circumstances, maintenance and retrofit interventions are needed to recover any loss of structural integrity (D'Ayala *et al.* 2013, Sorrentino *et al.* 2019, Chieffo *et al.* 2023). The integration of Structural Health Monitoring (SHM) systems in masonry structures becomes pivotal for the early detection of potential anomalies in their structural performance during their operating conditions, and thus even for the optimization of maintenance/retrofit interventions (Mesquita *et al.* 2017, Gentile *et al.* 2019, Limongelli 2020, Adam *et al.* 2022). Among the diverse SHM strategies, strain-based SHM approaches are widely recognized by the scientific community for their effectiveness in detecting localized/small structural damage that can develop in masonry structures (Glisic 2022). Nonetheless, their applications to real structural settings are still rather limited nowadays, largely due to scalability issues affecting the strain-sensing technologies currently available on the market. In a context where the research community is focusing on developing new sensing technologies and approaches for smart SHM of civil structures and infrastructures (Laflamme *et al.* 2023), recently, innovative clay-based smart sensors, termed "smart bricks," were developed by the Authors with the goal of achieving large-scale implementation of SHM systems in masonry structures. Smart bricks are piezoresistive strain-sensing brick-like sensors (Meoni *et al.* 2020) that, due to their similarity to traditional clay bricks, can be easily installed within new/existing masonry load-bearing structures to achieve diffuse strain monitoring during their operating conditions. Nowadays, the effectiveness of smart bricks for monitoring strain in masonry structures has been demonstrated by testing them in different structural contexts under laboratory conditions (see Meoni *et al.* 2019, Meoni *et al.* 2021b, and Meoni *et al.* 2023). However, applications to realistic masonry buildings, for instance exposed to changing environmental conditions, are still in progress.

In this sense, this paper presents an experimental campaign in which smart bricks are employed for the first time to monitor strain within a full-scale masonry building prototype subjected to controlled damage under real environmental conditions. In particular, the effectiveness of smart bricks for measuring strain in such a real-world scenario was preliminarily investigated by exploiting data collected during the execution of a load test carried out on the building mockup. The paper is organized as follows. Section 2 briefly recalls the smart brick technology. Section 3 outlines the experimental methodology by providing details on the construction of the building mockup and its SHM system. The methodology adopted to conduct the load test on the structure is also reported along with the processing of the data collected during the experiment. Section 4 presents the results obtained from the performed load test, while Section 5 concludes the paper with comments and remarks.

2. Smart bricks

A sample of smart brick is schematically represented in Fig. 1(a). These innovative strain-sensing sensors are produced like traditional clay bricks, yet by adding a specific amount of stainless-steel microfibers (a 1D electrically conductive filler) to the fresh clay matrix to enhance the piezoresistive capability of the clay-based material. At the end of the production process, smart bricks are equipped with thin external copper plate electrodes to perform electrical measurements. An insulating layer is also applied to the smart bricks to cover their outer surfaces and those of the copper electrodes, thus limiting electrical interference from other masonry components in the electrical outputs. A detailed description of the production process of smart bricks can be found in Meoni *et al.* (2020). Because of the improved piezoresistive capability, smart bricks can provide measurable changes in their electrical resistance, R, when mechanically strained under compression (or decompression). Specifically, an increase in the compressive strain state of a smart brick results in a decrease in its electrical resistance. Electrical outputs from smart bricks can be converted into mechanical axial strain (positive in compression), ε, by using the electromechanical model in Eq. (1) from Meoni *et al.* (2020):

$$\frac{\Delta R}{R_{i,0}} = \frac{R - R_{i,0}}{R_{i,0}} \cong a'\varepsilon^{-b} - \lambda\varepsilon \tag{1}$$

where a' is the relative sensing at the contact interfaces between the surfaces of smart bricks and their electrodes, b is a positive constant referred to as the contact resistance, $R_{i,0}$ is the unstrained internal electrical resistance of the smart bricks, and λ represents the gauge factor, which expresses the piezoresistive capability. Due to their similarity to traditional clay bricks, smart bricks can be easily placed at strategic positions within the load-bearing structure of a masonry building to monitor changes in strain due to damage initiation and propagation, as conceptually illustrated in Fig. 1(b). Anomalies in the structural performance of the monitored structure can be detected through the assessment of modifications in the strain outputs of each smart brick included in the sensor network with respect to the reference strain values measured when the monitored structure was undamaged. An experimental application of this monitoring strategy can be found in Meoni *et al.* (2019). In the case of implementation in historical buildings, where smart bricks are incorporated into the structural context at the end of construction, reference strain values can be set in the early stages of monitoring system operation. Because of their limited invasiveness, smart bricks can be deployed within load-bearing structures even in dense sensor networks, thus resolving the scalability issues that plague traditional strain-sensing technologies.

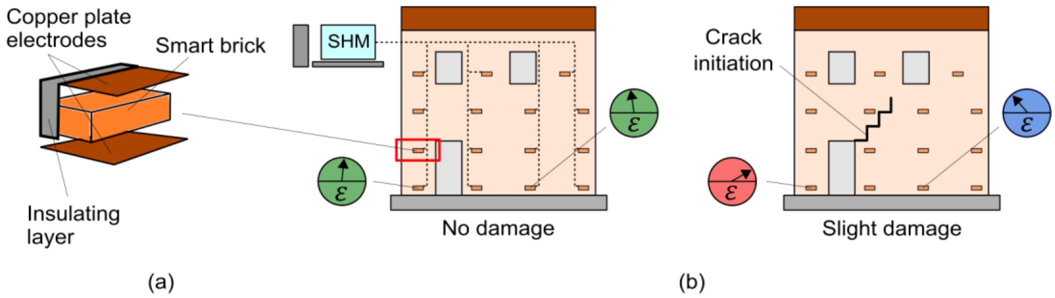

Figure 1. Smart bricks: (a) schematic representation of a sample; (b) conceptual exemplification of operation (changes in strain occurred due to the development of cracking patterns compared to the no damage condition).

3. Methodology

3.1 Masonry building prototype and monitoring system

The masonry building prototype object of the monitoring activities, represented in Fig. 2(a), consists of two stories with plan dimensions of 472 x 350 cm^2 and an overall height of 467 cm. The walls are 25 cm thick and were built by arranging clay bricks with 1 cm thick layers of lime mortar. The first slab consists of a 12.5-cm-thick polycentric masonry vault with a gravel fill. At the roof level, a one-way wooden slab, including five C24-type wooden beams, is present. Both the vault and the wooden slab are used to redistribute loads on Façades A and C. All openings of the building mockup have C24-type wooden lintels. Four S235 steel chains with a diameter of 18 mm were installed at the ground floor. Steel plates measuring 40 cm x 40 cm x 2.5 cm each are used to redistribute stresses at the ends of steel chains. Façades A, C, and D were built interconnected with each other, while 18 M8-type steel bars were embedded within the masonry to ensure the mechanical connection among Façades A, C, and B; this last Façade was constructed detached from the other masonry components by using a plastic film interface. Different degrees of connection between Façades A, C, and B will be simulated by acting on the tensioning of the steel bar system. The building mockup has steel beam foundations; these were properly designed to mechanically simulate differential settlements on the part of the foundation under Façade D. Simulation of different degrees of connection between Façades A, C, and B, as well as differential foundation settlements, represent some of the controlled damage that will be imposed on the building mockup. An integrated sensor network for continuous strain monitoring, consisting of 13 smart bricks of 250 x 55 x 120 mm^3, produced with the 0.25% of stainless-steel microfibers relative to the weight of the fresh clay matrix, was implemented on the building mockup since its construction phase. The novel sensors were installed within the masonry load-bearing structure as if they were traditional clay bricks. The positioning of smart bricks is schematically depicted in Fig. 2(b). A multichannel strain measurement technique, initially developed for smart concrete sensors (Meoni *et al.* 2021a), is adopted to perform electrical measurements on smart bricks every 10 minutes for a duration of 10 seconds. The novel sensors are powered with a voltage square wave input of 20 V peak-to-peak, duty cycle of 50%, and frequency of 1 Hz, while simultaneous voltage measurements are carried out on their reference resistor with a sample rate of 10 Hz. Once determined the electrical resistance of each smart brick (see Meoni *et al.* 2023 for details on the processing of the electrical outputs), strain measurements were retrieved by using Eq. (1) specialized with the parameters collected in Table 1. It is worth mentioning that the reported parameters were determined by performing electromechanical tests on several smart bricks in laboratory conditions. A Tinytag data logger was deployed at the ground floor of the building mockup to measure air temperature and relative humidity every 10 minutes. The so-composed monitoring system has been operational since March 9th, 2021.

Table 1. Parameters adopted to specialize Eq. (1) for the retrieval of strain measurements from the processing of electrical outputs of smart bricks ($R_{i,0}$ is the unstrained internal electrical resistance of smart bricks, α' is the relative sensing at the contact interfaces between the surfaces of smart bricks and their electrodes, b is a positive constant referred to the contact resistance, and λ represents the gauge factor).

$R_{i,0}$ [Ω]	α' [-]	b [-]	λ [-]
1.96E+07	4.70E-08	2.16	1603

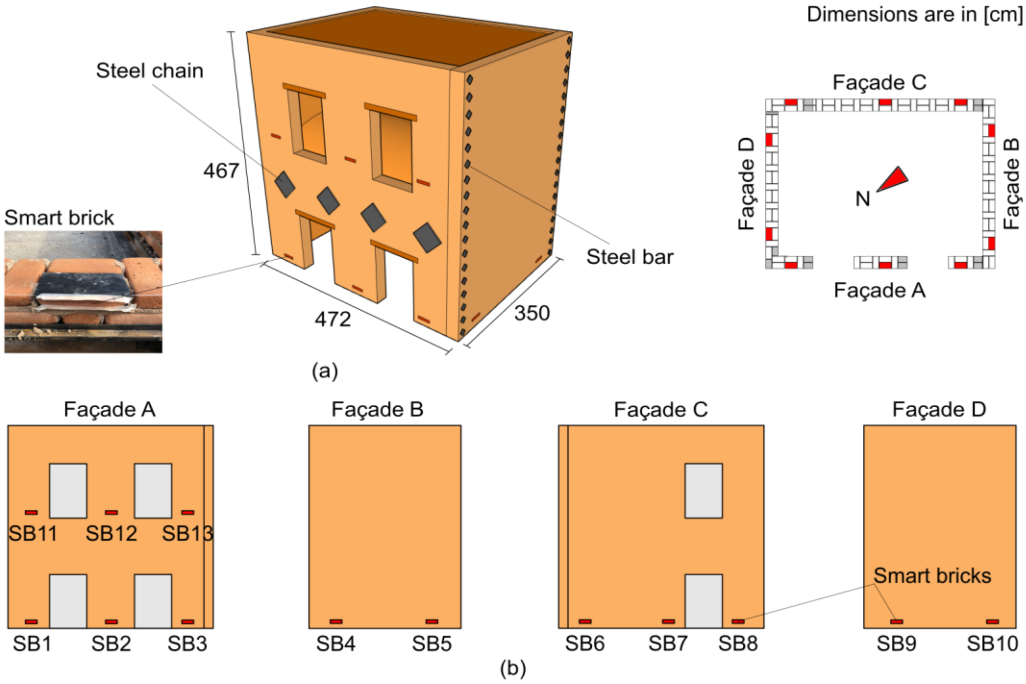

Figure 2. Masonry building prototype: (a) schematic representation; (b) positioning of smart bricks.

3.2 Experimental test and data processing

Once the construction of the building mockup was completed, additional live loads were added to the structure at multiple steps. On July 21st, 2021, a mass of 3.2 tons, consisting of concrete building material scraps, such as old beam specimens, was distributed on the slab at the roof level. The loading phase began at 8:00 a.m. and ended at 12:30 p.m. Considering the entity of the applied live loads and the one-way slab at the roof level, the strain increment expected on each smart brick embedded within Façades A and C was determined through manual calculation based on simplifying assumptions. Smart bricks' strain measurements collected within the duration of the load test were inspected to assess the sensitivity of the novel sensors to such an increase in live loads. Given the duration of the test and the susceptibility of smart bricks' outputs to changes in environmental conditions (Meoni *et al.* 2022), strain measurements collected from the novel sensors, ε, were further processed to remove potential trends due to the influence of changes in air temperature and relative humidity. With this purpose, a Multiple Linear Regression (MLR) model was taken into consideration to predict fluctuations in smart bricks' strain measurements due to environmental effects, ε_{env}, as follows:

$$\varepsilon_{env} = \beta_0 + \beta_1 \cdot T + \beta_2 \cdot H + e \tag{2}$$

where β_0, β_1, and β_2 represent the regression coefficients, T and H are the values of the air temperature and relative humidity, respectively, hence e represents the residual error of the regression model. The MLR model was preferred to the compensated electromechanical model developed in Meoni *et al.* 2022 to retrieve strain measurements from smart bricks under changing environmental conditions as further investigation is needed to apply the latter model to real-world scenarios. Regression coefficients were estimated for every smart brick in the sensor network by considering strain outputs and environmental data acquired when the building mockup was in normal operating conditions. Specifically, smart bricks' strain measurements, air temperature outputs, and relative humidity values ranged from 8:00 a.m. on July 19th, 2021, to 8:00 a.m. on July 20th, 2021, were considered for the estimation of the regression coefficients. Correlations between experimental strain measurements from smart bricks, air temperature outputs, and relative humidity values were evaluated with Pearson's correlation index, while the quality of the fitting of the MLR model to the strain measurements was assessed via the coefficient of determination, R^2. The mean standard deviation of the residual errors of the MLR model was computed to quantify the minimum measurable strain from smart bricks after removal of environmental effects. Strains due to the applied live load, ε_{load}, compensated from the environmental effects were computed for each smart brick as follows:

$$\varepsilon_{load} = \varepsilon - \varepsilon_{env} \tag{3}$$

The changes in strain due to the application of live loads were calculated for each smart brick by using the following relationship:

$$\Delta\varepsilon = \varepsilon_{load} - \varepsilon_{load,0} \quad (4)$$

where $\varepsilon_{load,0}$ is the strain value measured by a smart brick slightly before the beginning of the load test (when the building mockup was in normal operating conditions).

4. Results

4.1 Estimation of the regression coefficients

Figure 3 shows examples of MLR model fitting to experimental strain measurements from smart bricks together with the air temperature and relative humidity values considered to feed the adopted regression model. A quite strong positive correlation between experimental strain and air temperature values is demonstrated; the average Pearson's correlation index is about 0.85. On the contrary, the correlation between strains and relative humidity values is negative and quite scarce, as indicated by the average Pearson's correlation index of about -0.35. Overall, the selected MLR model fits well with the experimental strain measurements retrieved from smart bricks. In fact, an average R^2 equal to 0.8600 was computed from the R^2 obtained by processing the data collected for every smart brick in the sensor network. To provide exemplifications of the MLR model fitting, Fig. 3(c) highlights the perfect agreement between the experimental and predicted strain outputs in the case of smart brick SB7 (best fitting in the series), whereas Fig. 3(d) shows the rather weak fitting of the model to data from smart brick SB11(worst fitting in the series). In this last case, the scattering trend affecting the strain measurements retrieved from smart brick SB11 certainly adversely affected the fit of the MLR model to the experimental data. Figs. 3(e) and 3(f) point out the values of the MLR model's residual error determined for both the proposed examples. After calculating residuals for the other smart bricks in the sensor network, a mean standard deviation of 1.0338E-05 was determined, which represents the minimum average measurable strain from the novel sensors after removal of environmental effects. Figs. 3(g) and 3(h), showing the histogram of the residuals in the case of smart bricks SB7 and SB11, respectively, highlight the distribution of the variance of the model's residual error, the latter being sufficiently characterized by a normal distribution, especially in the case of smart brick SB7, as expected. Lastly, Table 2 collects the regression coefficients estimated for every smart brick in the sensor network from the fitting procedure. In agreement with the obtained values of Pearson's correlation index, the assessment of β_1 and β_2 values puts in evidence the greater contribution of the changes in air temperature in the estimation of ε_{env} compared to the changes in relative humidity (values of β_1 are generally an order of magnitude higher than those of β_2).

Table 2. Regression coefficients estimated for every smart brick included in the sensor network.

Smart brick	$\boldsymbol{\beta_0}$ **[-]**	$\boldsymbol{\beta_1}$ **[1/°C]**	$\boldsymbol{\beta_2}$ **[1/%]**	**Smart brick**	$\boldsymbol{\beta_0}$ **[-]**	$\boldsymbol{\beta_1}$ **[1/°C]**	$\boldsymbol{\beta_2}$ **[1/%]**
SB1	6.35E-04	3.55E-06	-2.12E-07	SB8	-9.48E-04	3.15E-05	8.45E-06
SB2	4.61 E-04	7.95E-06	2.09E-07	SB9	-6.74E-04	2.72E-05	4.60e-06
SB3	-4.97E-05	2.09E-05	4.63E-07	SB10	1.32 E-04	1.47E-05	2.64E-06
SB4	-9.68E-05	1.93E-05	2.59E-06	SB11	2.68 E-04	4.58E-06	-8.27E-07
SB5	2.14E-04	1.40E-05	2.02E-06	SB12	6.31 E-04	3.74E-06	-2.47E-07
SB6	4.70E-04	7.63E-06	2.65E-07	SB13	-1.83 E-04	1.94E-05	1.97E-06
SB7	1.41E-04	1.60E-05	2.35E-06				

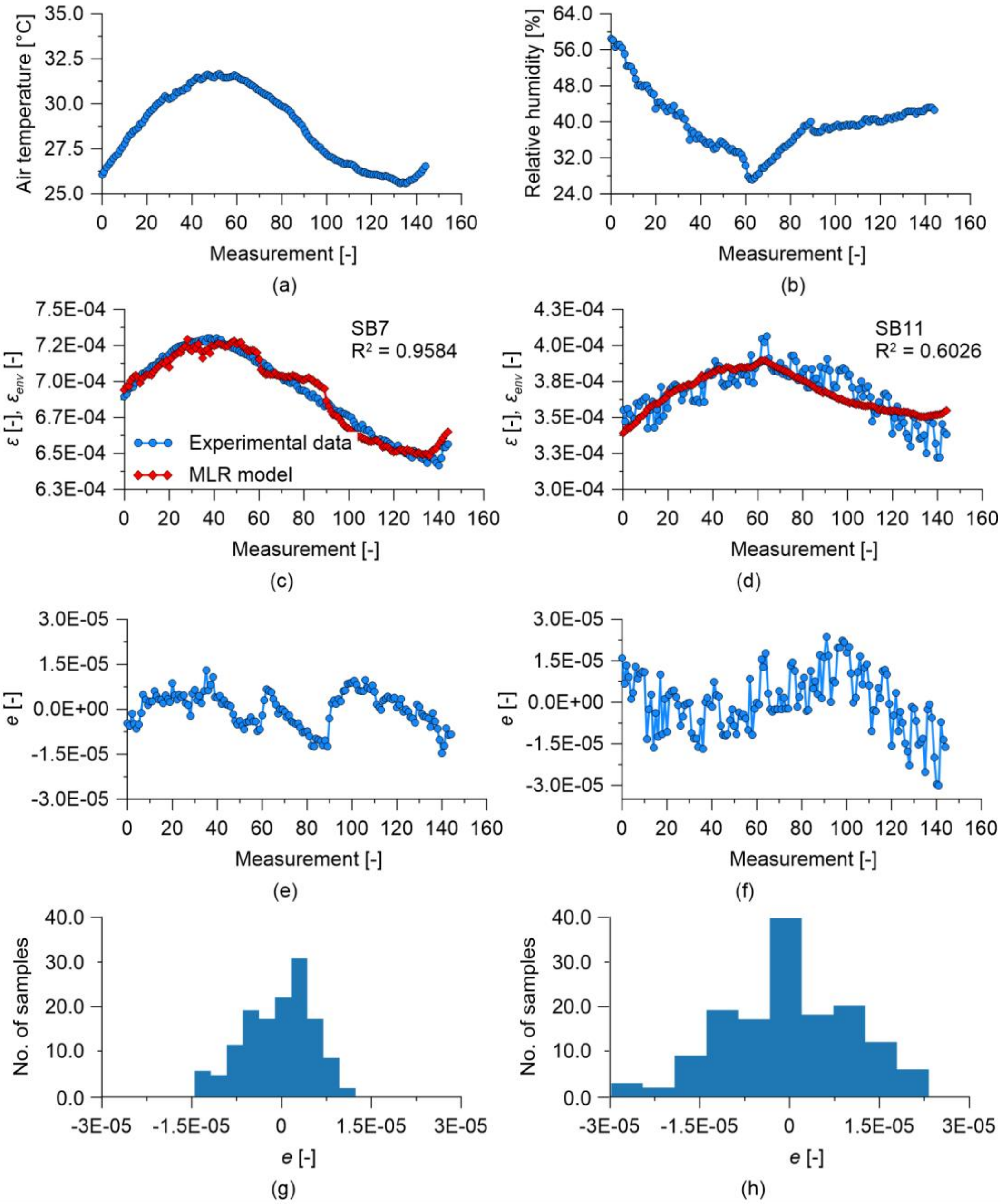

Figure 3. Examples of MLR model fitting to experimental strain measurements from smart bricks together with the air temperature and relative humidity values considered to feed the selected regression model: (a) air temperature trend; (b) relative humidity trend; (c) smart brick SB7 (best fitting in the series); (d) smart brick SB11 (worst fitting in the series); (e) MLR model's residual error determined for smart brick SB7; (f) MLR model's residual error determined for smart brick SB11; (g) histogram of the residual error determined for smart brick SB7; (h) histogram of the residual error determined for smart brick SB11.

4.2 Detection of the strain increment due to the load test

A slight strain increment of about 3.7E-06 was expected on each smart brick embedded within Façades A and C at the end of the load test, based on manual calculation. Fig. 4 illustrates the data collected during the execution of the load test. Air temperature increased from about 26°C to 32°C during the experiment (see Fig. 4(a)), following a linear trend like that characterizing the first branch of the temperature data in Fig. 3(a). Similarly, the relative humidity values collected during the load test (see Fig. 4(b)) are comparable in value to the outputs in the first branch of the plot in Fig. 3(b). As a result, considering the outcomes from Section 4.1, at least part of the increasing trend characterizing the strain measurements reported in Fig. 4(c) can be attributed to the changing environmental conditions rather than solely to the effect of the applied live loads.

Fig. 5 shows the changes in strain measured by smart bricks during the load test after the removal of environmental effects. Measurements from smart bricks positioned at the first floor of Façade A (smart bricks SB11, SB12, and SB13) were purposely omitted from this image as their trends resemble those reported without adding new information. Overall, the novel sensors outputted changes in strain of greater magnitude than expected. In addition, comparing strain values collected at the beginning and end of the load test, some of the reported trends indicate stable strain conditions (see smart bricks SB5, SB7, and SB9), while most denote the occurrence of decompression phenomena on the novel sensors (see, for example, smart bricks SB1, SB2, and SB3), which is hardly compatible with the type of test performed on the building mockup (in fact, a general increase in strain was expected). Conceivably, trends shown in Fig. 5 are the result of intrinsic noise affecting the outputs of smart bricks after the removal of environmental effects. In fact, the reported changes in strain measured by smart bricks are comparable in value with the minimum average measurable strain from the novel sensors determined in the previous section. Since the expected strain increment was less than the level of residual noise in smart bricks' strain measurements, it is reasonable that the novel sensors could not reveal the changes in strain imposed by the application of the live loads on the wooden slab of the building mockup. Overall, however, the presented signal processing method is ready to be used for detecting future changes in strain within the mockup caused by artificially imposed damage, having largely removed the effects of changing environmental conditions.

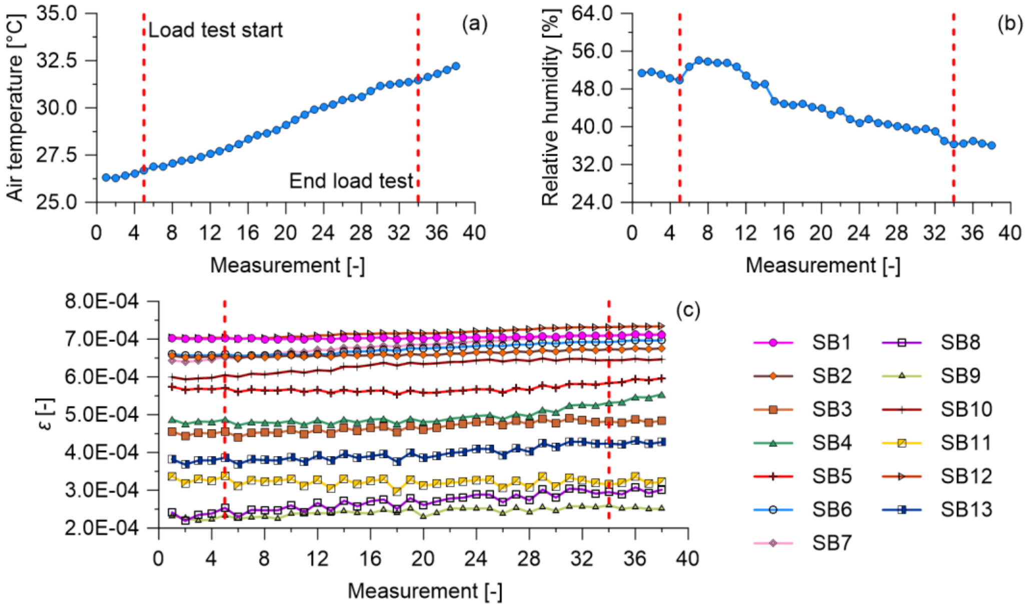

Figure 4. Data collected during the execution of the load test: (a) air temperature; (b) relative humidity; (c) smart bricks' strain measurements.

5. Conclusions

The paper presented an experimental program in which smart bricks, a novel class of strain-sensing sensors for SHM of new and existing masonry buildings, were integrated within the load-bearing structure of a full-scale masonry building prototype during its construction for strain monitoring. The structure will be subjected to several controlled damage scenarios during its operating conditions to induce damage of increasing entities. Smart bricks will be used for the monitoring of damage-induced changes in strain, and thus to detect and localize the onset of structural disruptions and collapse mechanisms.

The effectiveness of smart bricks for measuring strain in such a real structural context was preliminarily investigated by exploiting data collected during the execution of a load test carried out on the building mockup after the completion of its construction. Specifically, additional live loads were gradually positioned on the wooden slab at the roof level of the structure. Throughout the duration of the load test, strain measurements were retrieved from the processing of the electrical outputs from smart bricks, hence air temperature and relative humidity values were collected from a Tinytag data logger. Strain outputs from smart bricks were compensated by environmental effects, i.e., changing temperature and humidity conditions, by using a selected regression model, then the so-obtained strain trends were assessed and compared with the strain increment expected due to the application of the live loads; this last strain value was determined via simplified manual calculation. The obtained results indicate that the expected strain increment was about 3.7E-06. Smart bricks were therefore subjected to a very slight increase in strain during the performed load test, which could not be detected. This is a possible outcome from the performed load test because nowadays published literature indicates the use of smart bricks to measure strain values an order of magnitude higher than the strain increment expected in this test. In addition, the expected change in strain is found to be smaller than the mean standard deviation of the residual noise after removing environmental effects which is here quantified in about 1.0338E-05. Future studies will focus on adopting more refined algorithms to compensate strain measurements of smart bricks from environmental effects, as well as using the novel sensors to detect damage-induced changes in strain following the execution of damage scenarios involving the building mockup in the next phases of the experimental program.

Acknowledgements

The Authors acknowledge the Italian Ministry of University and Research (MUR) for financially supporting the reported research activities through the PRIN-2017 project DETECT-AGING (Project code 201747Y73L). The first Author also acknowledges the European Union - NextGenerationEU and the University of Perugia for supporting the work through the project Vitality framed within the National Innovation Ecosystem Grant ECS00000041. The authors also acknowledge support from the Italian Ministry of University and Research (MUR) through the FIS-2021 project “Smart Masonry enabling SAFEty-assessing STructures after earthquakes (SMS-SAFEST)” (Project code FIS00001797).

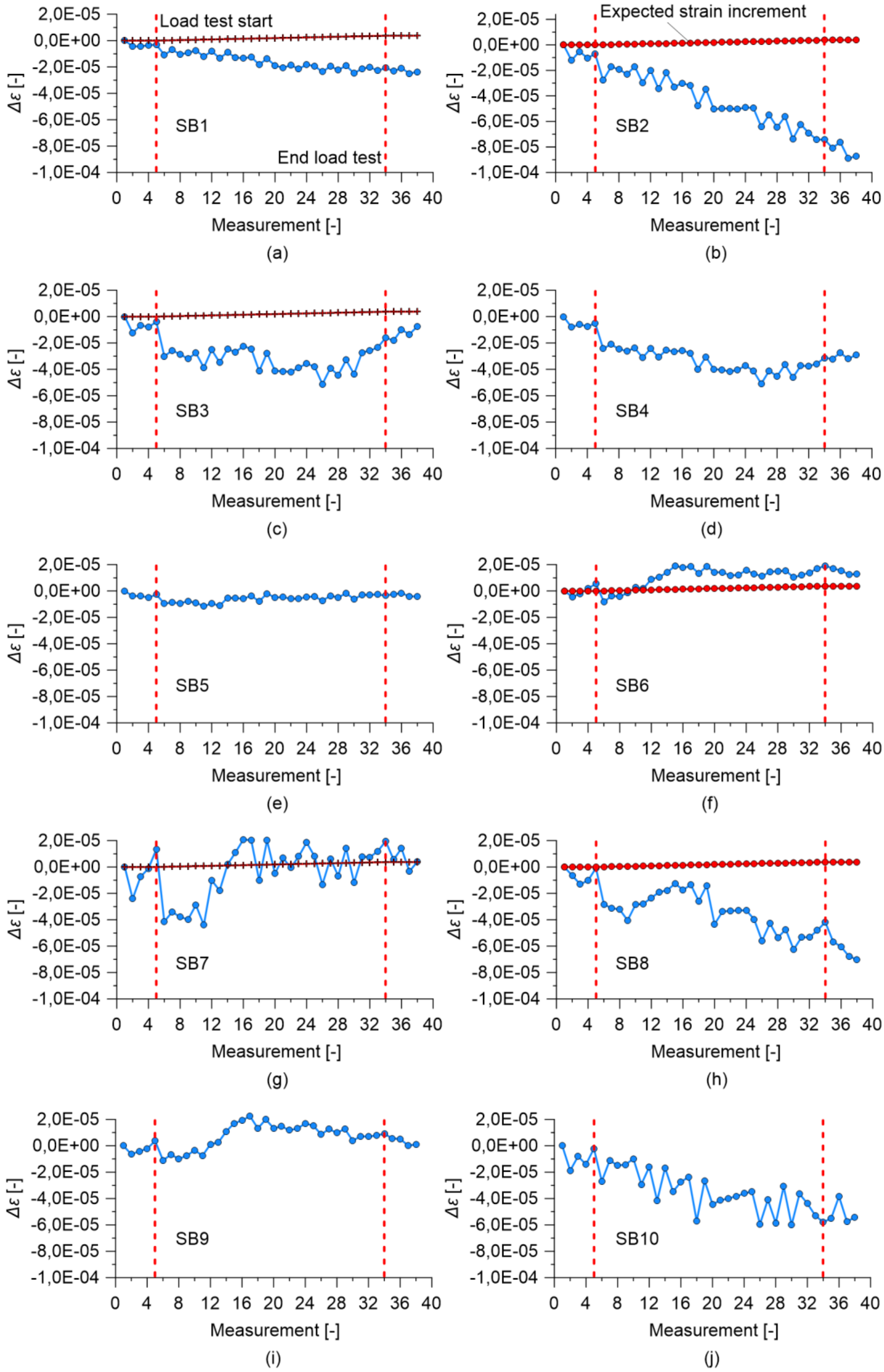

Figure 5. Changes in strain measured by the smart bricks embedded at the ground floor of the building mockup following the application of live loads, with annotated the expected strain increment on smart bricks embedded within the Façades A and C.

References

Adam, J.M., Betti, M., Clementi, F. and Ivorra, S., 2022. Structural health monitoring and NDT of masonry structures: Research and practice. Construction and Building Materials, p.125704.

Chieffo, N., Formisano, A. and Lourenço, P.B., 2023, February. Seismic vulnerability procedures for historical masonry structural aggregates: Analysis of the historical centre of Castelpoto (South Italy). In Structures (Vol. 48, pp. 852-866). Elsevier.

D'Ayala, D., 2013. Assessing the seismic vulnerability of masonry buildings. In Handbook of seismic risk analysis and management of civil infrastructure systems (pp. 334-365). Woodhead publishing.

Gentile, C., Ruccolo, A. and Canali, F., 2019. Continuous monitoring of the Milan Cathedral: dynamic characteristics and vibration-based SHM. Journal of Civil Structural Health Monitoring, 9, pp.671-688.

Glisic, B., 2022. Concise historic overview of strain sensors used in the monitoring of civil structures: The first one hundred years. Sensors, 22(6), 2397.

Limongelli, M.P., 2020. SHM for informed management of civil structures and infrastructure. Journal of Civil Structural Health Monitoring, 10, pp.739-741.

Meoni, A., D'Alessandro, A., Mancinelli, M., and Ubertini, F., 2021a. A multichannel strain measurement technique for nanomodified smart cement-based sensors in reinforced concrete structures. Sensors, 21(16), 5633.

Meoni, A., D'Alessandro, A. and Ubertini, F., 2020. Characterization of the strain-sensing behavior of smart bricks: A new theoretical model and its application for monitoring of masonry structural elements. Construction and Building Materials, 250, p.118907.

Meoni, A., D'Alessandro, A., Cavalagli, N., Gioffré, M. and Ubertini, F., 2019. Shaking table tests on a masonry building monitored using smart bricks: Damage detection and localization. Earthquake Engineering & Structural Dynamics, 48(8), pp.910-928.

Meoni, A., D'Alessandro, A., Kruse, R., De Lorenzis, L. and Ubertini, F., 2021b. Strain field reconstruction and damage identification in masonry walls under in-plane loading using dense sensor networks of smart bricks: Experiments and simulations. Engineering Structures, 239, p.112199.

Meoni, A., D'Alessandro, A., Saviano, F., Lignola, G.P., Parisi, F. and Ubertini, F., 2023. Strain Monitoring and Crack Detection in Masonry Walls under In-Plane Shear Loading Using Smart Bricks: First Results from Experimental Tests and Numerical Simulations. Sensors, 23(4), p.2211.

Meoni, A., Fabiani, C., D'Alessandro, A., Pisello, A. L., & Ubertini, F., 2022. Strain-sensing smart bricks under dynamic environmental conditions: Experimental investigation and new modeling. Construction and Building Materials, 336, 127375.

Mesquita, E., Arêde, A., Silva, R., Rocha, P., Gomes, A., Pinto, N., Antunes, P. and Varum, H., 2017. Structural health monitoring of the retrofitting process, characterization, and reliability analysis of a masonry heritage construction. Journal of Civil Structural Health Monitoring, 7(3), pp.405-428.

Laflamme, S., Ubertini, F., Di Matteo, A., Pirrotta, A., Perry, M., Fu, Y., ... & Milillo, P., 2023. Roadmap on measurement technologies for next generation structural health monitoring systems. Measurement Science and Technology.

Sorrentino, L., Cattari, S., Da Porto, F., Magenes, G. and Penna, A., 2019. Seismic behaviour of ordinary masonry buildings during the 2016 central Italy earthquakes. Bulletin of Earthquake Engineering, 17(10), pp.5583-5607.